

HIGH-ENERGY PROCESSES IN YOUNG STARS: *CHANDRA* X-RAY SPECTROSCOPY OF HDE 283572, RY TAU, AND LkCa 21

M. Audard¹, S. L. Skinner², K. W. Smith³, M. Güdel⁴, and R. Pallavicini⁵

¹Columbia Astrophysics Laboratory, Columbia University, Mail code 5247, 550 West 120th Street, New York, NY 10027, USA

²Center for Astrophysics and Space Astronomy, University of Colorado, Boulder, CO 80309-0389, USA

³Max-Planck-Institut für Radioastronomie, Auf dem Hügel 69, 53121 Bonn, Germany

⁴Paul Scherrer Institut, Villigen & Würenlingen, 5232 Villigen PSI, Switzerland

⁵Osservatorio Astronomico di Palermo, Piazza del Parlamento 1, 90134 Palermo, Italy

ABSTRACT

Weak-lined T Tauri stars (WTTS) represent the important stage of stellar evolution between the accretion phase and the zero-age main sequence. At this stage, the star decouples from its accretion disk, and spins up to a higher rotation rate than in the preceding classical T Tauri phase. Consequently, dynamo processes can be expected to become even stronger at this stage. High energy processes can have effects on the remaining circumstellar material, possibly including protoplanets and planetesimals, and these effects may account for certain observable properties of asteroids in the current solar system. *Chandra* observed for 100 ks the WTTS HDE 283572 which probes the PMS stage of massive A-type stars. We present first results of the analysis of its high-resolution X-ray spectrum obtained with the High-Energy Transmission Grating Spectrometer. A wide range of Fe lines of high ionization states are observed, indicating a continuous emission measure distribution. No significant signal is detected longward of the O VIII Ly α line because of the high photoelectric absorption. We also report on the preliminary analysis of the zeroth order spectra of RY Tau and LkCa21. In particular, we show evidence of an emission line in RY Tau at 6.4 keV that we identify as fluorescent emission by neutral Fe caused by a strong X-ray flare which illuminated some structure in (or surrounding) the CTTS. A comparison of X-ray spectra of classical T Tau stars, other WTTS, and young main-sequence stars is made.

in WTTS are thought to originate from magnetic activity due to a dynamo mechanism similar to main-sequence magnetically active stars. While accretion disks in CTTS keep the rotation rate low, the highest rotation rates occur in WTTS, due to the dispersion of the disk. Magnetic activity is thus very strong in these PMS stars ($10^{28.5} - 10^{31}$ erg s⁻¹). WTTS are, therefore, most important for our deeper understanding of extreme magnetic activity in young stars, of the evolution of the circumstellar envelope and disk, and of the formation of planetary systems (e.g., Feigelson & Montmerle 1999).

The origin of X-ray emission in young PMS stars still remains unclear. X-ray grating spectroscopy of accretion-fed CTTS have shown stimulating, but conflicting results: TW Hya, a nearby CTTS seen pole-on, showed a soft X-ray spectrum (3 MK) with high densities ($\log n_e \sim 13$ cm⁻³; Kastner et al. 2002; Stelzer & Schmitt 2004), whereas another CTTS, SU Aur, displayed a spectrum characteristic of a dominant very hot plasma ($T \sim 30 - 50$ MK; Skinner & Walter 1998; Smith et al. 2005). Whereas accretion has been claimed as the mechanism at the origin of X-rays in TW Hya, enhanced solar-like coronal activity appears to explain the X-ray spectrum of SU Aur. Although X-ray studies of CTTS are interesting, the lack of significant accretion in WTTS makes the latter excellent candidates to study magnetic activity in PMS stars.

2. TARGETS AND OBSERVATIONS

Chandra observed the WTTS star HDE 283572 with ACIS-S and the High-Energy Transmission Grating for 102 ks from October 20, 2003 (14h45m17s UT) to October 21, 2003 (19h37m43s UT). The nearby (8.5' separation) WTTS LkCa 21 was detected in the zeroth order image only, whereas the CTTS RY Tau was bright enough to produce significant signal in the grating arms as well. Table 1 gives some properties of the targets.

Our targets lie in the Taurus-Auriga star-forming region at $d \sim 140$ pc. The main target, HDE 283572, was discovered in X-rays and studied in detail by Walter et al. (1987) and later by Favata et al. (1998a). Its age and spectral type suggest that it is a probable predecessor of an A-type main-sequence star (Favata et al. 1998b). It rotates fast ($v \sin i \sim 80$ km s⁻¹; Johns-Krull 1996) and it is probably observed equator-on, implying a short rotation pe-

Key words: Stars: activity – Stars: coronae – Stars: individual: HDE 283572 – Stars: individual: RY Tau – Stars: individual: LkCa 21 – Stars: pre-main sequence – X-rays: stars

1. INTRODUCTION

Weak-lined T Tauri stars (WTTS) are of special interest for the study of magnetic activity in the early stages of a star. WTTS are pre-main sequence (PMS) stars between the accreting phase of a classical T Tau star (CTTS) and the disk-free phase of a zero-age main sequence (ZAMS) star. While the X-ray properties of protostars and CTTS may be related to the phenomenon of accretion, X-rays

Table 1. Target properties.

	HDE 283572	HD 283571	LkCa 21
A.k.a.	V987 Tau	RY Tau	V1071 Tau
SED class	III	II	III
Spectral type	G5 IV ^a	F8 III ^b	M3 ^c
Age (Myr)	3 ^c	1.6 ^d	0.5 ^e
Mass (M_{\odot})	1.8 ± 0.2^a	1.4^f	0.2^e
$v \sin i$ (km/s)	78 ± 1^a	55 ± 3^b	60 ± 11^g
P_{rot} (d)	$1.55^{a,h}$
A_V (mag)	$0.4 - 0.6^a$	2.7^i	0.65^c
$\log N_{\text{H}}$ (10^{21} cm^{-2})	20.60^j	21.70^j	$< 21.3^j$
$\log L_X$ (erg/s)	31.14^j	30.88^j	29.83^j

References: ^aStrassmeier & Rice (1998),
^bMora et al. (2001), ^cDamiani et al. (1995),
^dHartigan et al. (1995), ^eMartín et al. (1994),
^fBasri et al. (1991), ^gHartmann et al. (1987),
^hWalter et al. (1987), ⁱBeckwith et al. (1990), ^jThis work

riod (Walter et al. 1987). In X-rays, HDE 283572 displays a dominant hot plasma (10 – 40 MK) and its light curves show evidence for rapid and intense flare-like variations (Favata et al. 1998a; Strom & Strom 1994; Stelzer et al. 2000). Both RY Tau and LkCa 21 lie about 8' north of HDE 283572 and were previously detected in X-rays (Damiani et al. 1995). Their X-ray fluxes are such that their count rates are about twenty times lower than that of HDE 283572. RY Tau was caught during the decay of a flare, and produced sufficient signal in the grating arms. However, the large off-axis distance significantly distorted the redistribution matrix thus degrading the spectral resolution of the grating spectra. Figure 1 shows the X-ray light curves in the HETGS first order (HDE 283572) and in zeroth order (RY Tau and LkCa 21).

3. DATA REDUCTION

The HETGS data were reduced with CIAO 3.0.2 and CALDB 2.26. We followed threads to produce a calibrated event type 2 file. In particular, we took care that events of RY Tau and LkCa 21 were properly calibrated. For HDE 283572, we assumed that no other contaminating source exists. While, in principle, order sorting could have differentiated crossing grating events of RY Tau (MEG +1) from those of HDE 283572 (HEG –1), this was not possible for this observation since both grating arms crossed at about the same energy. Thus, in the analysis below, we have discarded the 10.8 – 11.6 Å range in HEG –1.

4. SPECTRA

Figures 2 and 3 show the *Chandra* MEG first order spectra of RY Tau and HDE 283572, and the zeroth order spectra of RY Tau and LkCa 21, respectively. A few features can immediately be recognized by eye: i) the spectra

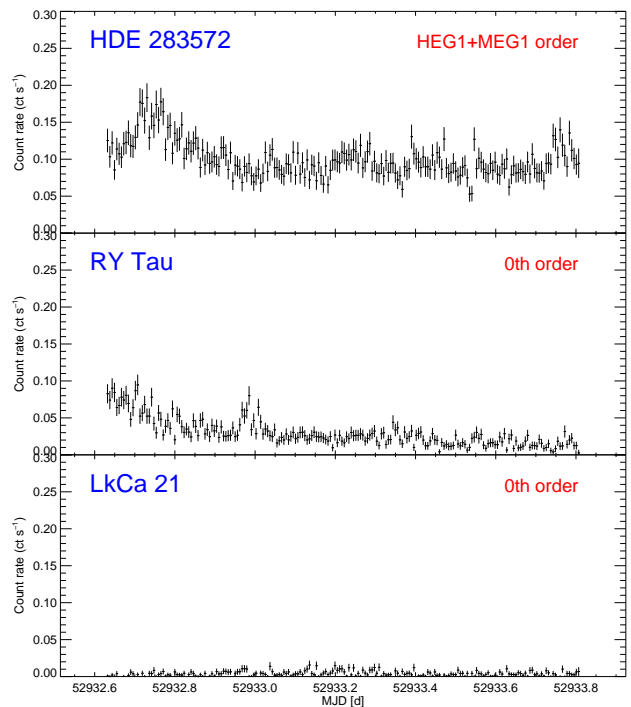


Figure 1. *Chandra* X-ray light curves of HDE 283572, RY Tau, and LkCa 21 (top, middle, and bottom panels). An identical vertical scale was used in each panel to emphasize the different X-ray fluxes. The count rate in the grating light curve of HDE 283572 is similar to that in the zeroth order.

of HDE 283572 and RY Tau both show a well-developed continuum at short wavelength, indicating a dominant hot plasma, with RY Tau being slightly hotter. ii) However, photoelectric absorption is much stronger in RY Tau than in HDE 283572. iii) A similar hydrogen column density can be found in the WTTS LkCa 21 and in the CTTS RY Tau. iv) The plasma in LkCa 21 is much cooler than in the other two targets. We present below preliminary results of our data analysis. Specifically, uncertainties are calculated as 20% of the best-fit values only; furthermore, whereas the grating spectra of HDE 283572 were analyzed, we fitted only the zeroth order spectra of RY Tau and LkCa 21. Solar photospheric abundances from Grevesse & Sauval (1998) are used here.

4.1. HDE 283572

We fitted simultaneously the HEG and MEG first positive and negative order spectra after rebinning to obtain a similar bin size of 20 mÅ. The negligible background was not subtracted allowing us to use the robust C statistics. We found that two absorbed isothermal collisional ionization equilibrium models could fit the data adequately. The best-fit parameters (with 20% quoted uncertainties) are $T_1 = 8.5 \pm 1.7$ MK, $T_2 = 23 \pm 4.6$ MK, $\text{EM}_1 = (3.3 \pm 0.7) \times$

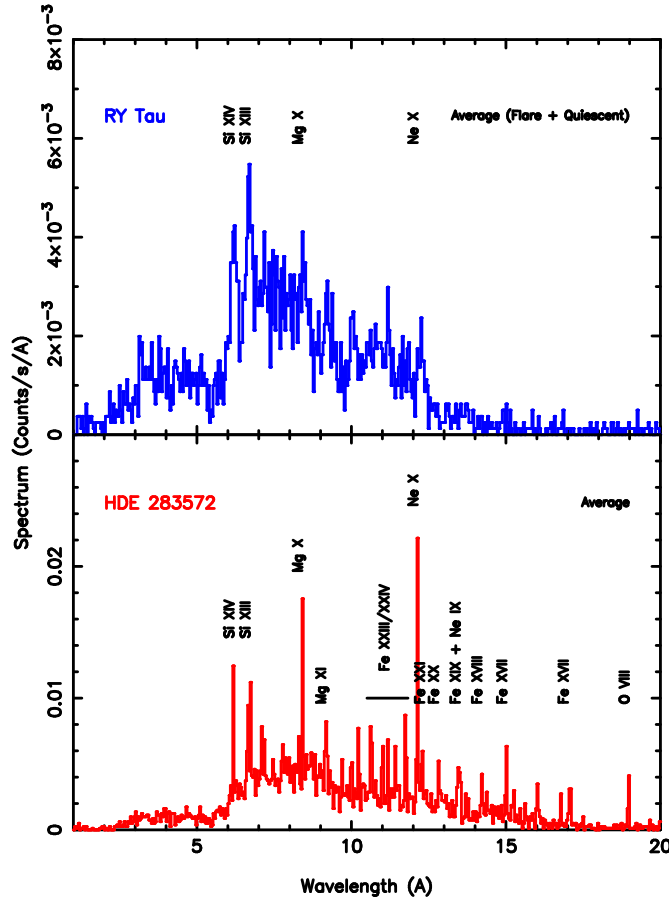


Figure 2. Chandra MEG first order average spectra of RY Tau (top) and HDE 283572 (bottom) with major emission lines labeled. Notice the strong continuum in both hot sources but the higher photoelectric absorption in the CTTS. The resolving power of the grating spectrum is also reduced at off-axis angles.

10^{53} cm^{-3} and $\text{EM}_1/\text{EM}_2 = 0.6$ ($\log L_X = 31.14 \text{ erg s}^{-1}$; $0.1 - 10 \text{ keV}$). We here fixed N_H to $4 \times 10^{20} \text{ cm}^{-2}$, i.e., the ROSAT PSPC value Favata et al. (1998a). This value is consistent with that obtained from a spectral fit to the zeroth order spectrum of HDE 283572. Coronal abundances were obtained as well: O = 0.48 ± 0.1 , Ne = 0.80 ± 0.16 , Mg = 0.41 ± 0.08 , Si = 0.35 ± 0.07 , S = 0.18 ± 0.04 , Ca = 1.12 ± 0.22 , Ar = 0.94 ± 0.19 , and Fe = 0.41 ± 0.08 . No additional component was required (C statistics of 3711 for 3230 degrees of freedom). However, this does not exclude the presence of a cooler component in HDE 283572. The photoelectric absorption in HDE 283572 prevented the detection of cooler plasma that could, e.g., be detected in the O VII triplet.

4.2. RY TAU

In this proceedings paper, we concentrate our analysis on the zeroth order spectrum of RY Tau. A 2- T model fit yields $T_1 = 12 \pm 2.4 \text{ MK}$, $T_2 = 45 \pm 9 \text{ MK}$, $\text{EM}_1 =$

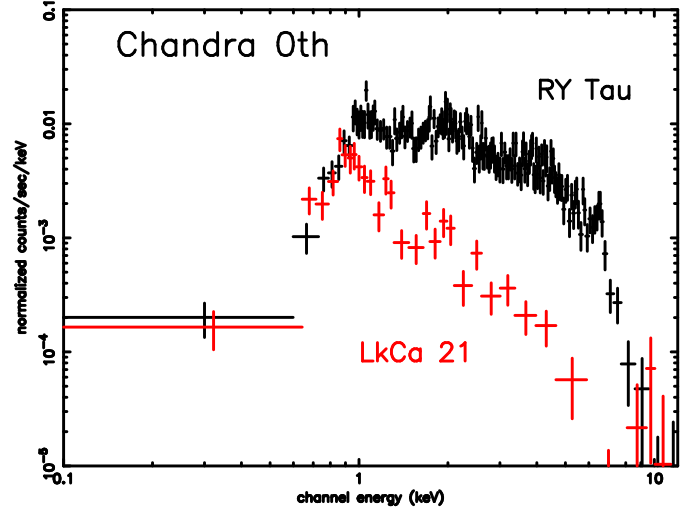


Figure 3. Chandra zeroth order average spectra of RY Tau (top) and LkCa 21 (bottom). Notice the similar photoelectric absorption at low energy but much hotter spectrum of RY Tau.

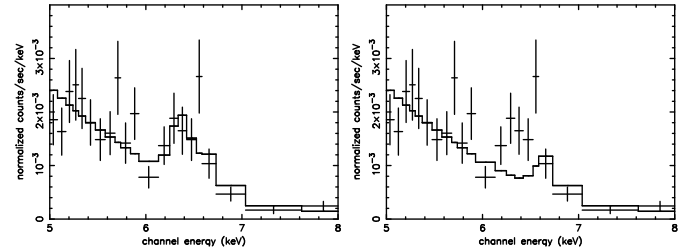


Figure 4. Zoom-in of the zeroth order spectrum of RY Tau around the Fe K line complex. An additional line component is required to fit a flux excess observed at 6.4 keV. A model with (left) and without (right) the emission line is shown.

$(1.9 \pm 0.4) \times 10^{53} \text{ cm}^{-3}$ and $\text{EM}_1/\text{EM}_2 = 0.5$ ($\log L_X = 30.88 \text{ erg s}^{-1}$; $0.1 - 10 \text{ keV}$). We obtained a global metallicity of $Z = 0.3 \pm 0.06$ and $N_H = (5 \pm 1) \times 10^{21} \text{ cm}^{-2}$. Most interestingly, an excess flux around 6.4 keV was observed in RY Tau. An additional emission feature with flux of $(4.3 \pm 1.9) \times 10^{-6} \text{ ph cm}^{-2} \text{ s}^{-1}$ (90% confidence range) was required. Figure 4 shows the high-energy region of the RY Tau spectrum with (left) or without (right) the additional component. This emission feature is reminiscent of fluorescent emission by Fe ions due to inner shell ionization of a 1s electron, and has been observed in the Sun (e.g., Neupert et al. 1967) and in young stellar objects (YSOs; Imanishi et al. 2001). The energy resolution of the ACIS detector does not allow us to determine the exact ionization state of the emitting ion; however, the line centroid ($6.37 \pm 0.05 \text{ keV}$) suggests that Fe II (originally Fe I before K-shell ionization), e.g., in the accretion disk, could well have fluoresced.

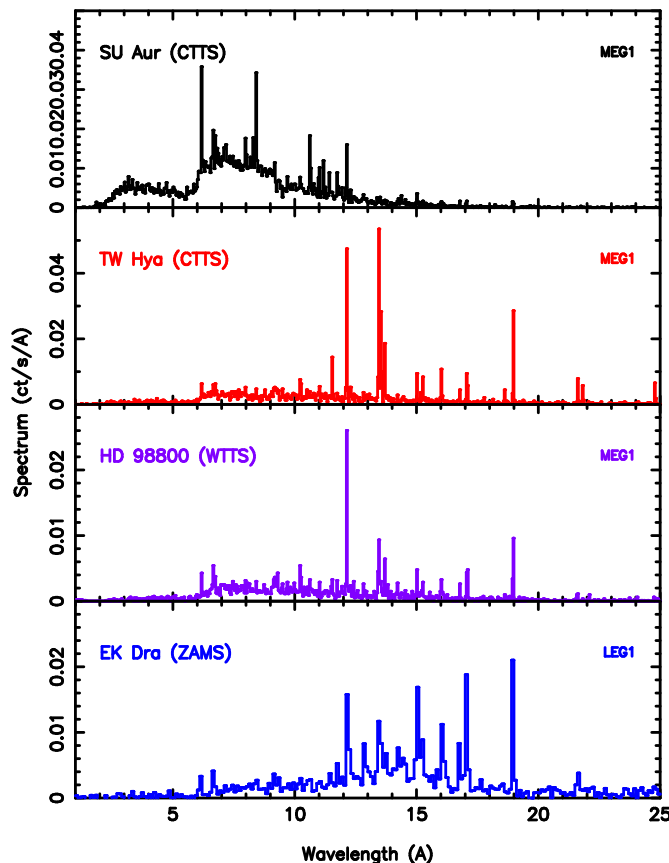


Figure 5. A sample of *Chandra* X-ray spectra of CTTS (SU Aur and TW Hya), WTTS (HD 98800), and ZAMS star (EK Dra).

4.3. LkCa 21

LkCa 21 was too faint for grating spectroscopy. A 2- T fit to the zeroth order spectrum yields $T_1 = 10 \pm 2$ MK, $T_2 = 25 \pm 5$ MK, $EM_1 = (0.35 \pm 0.07) \times 10^{53} \text{ cm}^{-3}$ and $EM_1/EM_2 = 1.2$, together with a global metallicity of $Z = 0.4 \pm 0.08$ and $N_H \leq 2 \times 10^{21} \text{ cm}^{-2}$ ($\log L_X = 29.83 \text{ erg s}^{-1}$; $0.1 - 10 \text{ keV}$). Thus this X-ray faint WTTS shows much cooler plasma than the brighter HDE 283572.

5. DISCUSSION

Figure 5 shows the *Chandra* X-ray spectra of CTTS SU Aur (age ~ 5 Myr; Smith et al. 2005), CTTS TW Hya (Kastner et al. 2002), WTTS HD 98800 (Kastner et al. 2004), and ZAMS star EK Dra (Telleschi et al. 2005). During the accretion phase, the CTTS in our sample display very hot plasmas (~ 30 MK), with the exception of TW Hya (age $\sim 5 - 10$ Myr) which shows cool plasma (3 MK). Again different spectra can be observed at the WTTS stage: whereas the corona of HD 98800 is cool (< 10 MK), HDE 283572's spectrum is similar to the hot CTTS. The ZAMS star EK Dra (age $\sim 50 - 70$ Myr) also shows a dominant cool plasma. In summary, no obvious trend can be seen from Class II to III in this small sample.

The detection of a fluorescence line in RY Tau may be explained by the flare observed in the X-ray light curve. It suggests that the X-ray flare source illuminated a cold structure, e.g., the accretion disk in RY Tau, and produced fluorescent emission after K-shell ionization by the hard X-ray photons. Further analysis will allow us to obtain some geometric constraints on the height of the X-ray source above the fluorescing material.

In conclusion, some CTTS display strong levels of magnetic activity; however, it remains unclear where TW Hya, because of its cool plasma and high electron densities, fits into this picture. Similarly, coronal emission measure distributions in WTTS are not unique. It remains unclear what properties dictate the X-ray emission in YSOs. Could it be age, rotation, stellar association, external conditions, etc. Hopefully, additional high-resolution X-ray spectra of PMS stars will shed light on this fundamental problem.

ACKNOWLEDGEMENTS

We acknowledge support from SAO grant GO3-4016X and from the Swiss NSF (grant 20-66875.01). The MIT/HETGS group is also thanked for insightful information on off-axis spectroscopy with *Chandra*.

REFERENCES

- Basri G., Martin E. L., Bertout C. 1991, A&A, 327, 625
- Beckwith S., Sargent A., Chini R. S., et al. 1990, AJ, 327, 924
- Damiani, F., Micela, G., Sciortino, S., et al. 1995, ApJ, 446, 331
- Favata, F., Micela, G., & Sciortino, S. 1998a, A&A, 337, 413
- Favata, F., Micela, G., Sciortino, S., & D'Antona, F. 1998, A&A, 335, 218
- Feigelson, E. D., & Montmerle, T. 1999, ARAA, 37, 363
- Grevesse, N., & Sauval, A. J. 1998, Space Science Reviews, 85, 161
- Hartigan P., Edwards S., Ghandour L. 1995, ApJ, 327, 736
- Hartmann, L. W., Soderblom, D. R., & Stauffer, J. R. 1987, AJ, 93, 907
- Imanishi, K., Koyama, K., & Tsuboi, Y. 2001, ApJ, 557, 747
- Johns-Krull, C. M. 1996, A&A, 306, 803
- Kastner, J. H., Huenemoerder, D. P., Schulz, N. S. 2002, ApJ, 567, 434
- Kastner, J. H., Huenemoerder, D. P., Schulz, N. S., et al. 2004, ApJ, 605, L49
- Martin, E. L., Rebolo, R., Magazzù, A., & Pavlenko, Y. V. 1994, A&A, 282, 503
- Mora, A., Merin, B., Solano, E., et al. 2001, A&A, 378, 116
- Neupert, W. M., Gates, W., Swartz, M., et al. 1967, ApJ, 149, L79
- Skinner, S. L., & Walter, F. M. 1998, ApJ, 509, 761
- Smith, K. W., Audard, M., Güdel, M., et al. 2005, these proceedings
- Stelzer, B., Neuhäuser, R., Hambaryan, V. 2000, A&A, 356, 949
- Stelzer, B. & Schmitt, J. H. M. M. 2004, A&A, 418, 687
- Strassmeier, K. G., & Rice, J. B. 1998, A&A, 339, 497
- Strom, K. M., & Strom, S. E. 1994, ApJ, 424, 237

- Telleschi, A., Güdel, M., Briggs, K., et al. 2005, these proceedings
- Walter, F. M., Brown, A., Linsky, J. L., et al. 1987, ApJ, 314, 297